

# Analysis of geomagnetic secular variation for the last 1.5 Ma recorded by volcanic rocks of the Trans Mexican Volcanic Belt: new data from Sierra de Chichinautzin, Mexico

A. Rodríguez-Trejo,<sup>1</sup> L. M. Alva-Valdivia,<sup>2</sup> M. Perrin,<sup>3</sup> G. Hervé<sup>3</sup> and N. López-Valdés<sup>1</sup>

<sup>1</sup>Posgrado en Ciencias de la Tierra, Instituto de Geofísica, Universidad Nacional Autónoma de México, Circuito de la Investigación Científica, C.P. 04510 México D. F., México. E-mail: [alekz.igf@hotmail.com](mailto:alekz.igf@hotmail.com)

<sup>2</sup>Laboratorio de Paleomagnetismo, Instituto de Geofísica, Universidad Nacional Autónoma de México, Circuito de la Investigación Científica, C.P. 04510 México D. F., México

<sup>3</sup>Aix Marseille Univ, CNRS, IRD, INRA, Coll France, CEREGE, Aix-en-Provence, France

Accepted 2019 July 5. Received 2019 June 16; in original form 2019 February 7

## SUMMARY

The great wealth of volcanism along the Trans Mexican Volcanic Belt (TMVB) and the need to improve the secular variation curve of the Earth magnetic field of the region is the aim of this research. 300 oriented cores from 33 sites and 21 individual cooling units were acquired from Sierra de Chichinautzin volcanic field (ChVF) and Sierra de Santa Catarina (SSC). Directional analysis and rock magnetic experiments were performed (e.g. thermal demagnetization, hysteresis loop, susceptibility vs temperature), achieving 21 new averaged palaeomagnetic directions. New results are consistent with the previous studies on the same cooling unit. We compiled all the palaeomagnetic studies performed on the ChVF, updating age and calculating an average direction per cooling unit and estimating an overall mean direction for the ChVF (Dec = 359.1°, Inc = 35.3°, N = 33, k = 21.6,  $\alpha_{95}$  = 5.5°, Plat = 87.7° N, Plong = 227.4° E, K = 31.8, A95 = 4.5°).

Afterwards, we compiled all the previous palaeomagnetic studies along the whole TMVB with age ranging from 0 to 1.5 Ma, and constrained the directional analyses by specific quality criteria such as well-defined age, number of samples and quality of kappa) on the cooling unit consistency.

The mean direction and virtual geomagnetic pole (VGP) estimated for the TMVB, during the periods 0–40 ka and 0–1.5 Ma, are close to the geographic pole, supporting the validity of the geocentric axial dipole hypothesis. The directional results of this study also fit well with the predictions at Mexico City of the models SHA.DIF.14k and CALS10k2 calculated for the last 14 ka. The dispersion of the VGP's on the TMVB are also consistent with the expected values proposed by different models of palaeosecular variation. However, large gaps in the temporal record remain that should be filled by further palaeomagnetic studies.

**Key words:** Palaeomagnetic secular variation; Rock and mineral magnetism.

## 1 INTRODUCTION

The Earth's magnetic field, mainly generated in the core of the Earth, has temporal and spatial variations in direction and intensity recorded by diverse geologic materials, as volcanic rocks, archaeological materials or sediments. However, sediments that can give only relative palaeointensity estimates will not be considered here. Global models were developed using data repositories, for example MagIC (<https://www2.earthref.org/MagIC>) or GEOMAGIA50.v3 (Brown *et al.* 2015), to characterize the behaviour and the variation through time of the geodynamo. For the last millennia, models as CALS10k.2 and ARCH10k.1 (Constable *et al.* 2016), SHA.DIF.14k

(Pavón-Carrasco *et al.* 2014) were computed by spherical harmonic analysis in space.

An accurate modelling requires a homogeneous spatial distribution of data over the globe. But the present distribution is strongly biased towards mid-latitudes of the northern hemisphere (e.g. Panovska *et al.* 2018), emphasizing the need of data from low latitudes and the Southern hemisphere. Mexico is a key area through its rich archaeological past and its intense and continuous volcanic activity for millions of years. Of particular interest, the TMVB is an active volcanic arc, characterized by thousands of volcanic structures that cross central Mexico from east to west (Fig. 1a). In the TMVB, two important volcanic fields were emplaced from

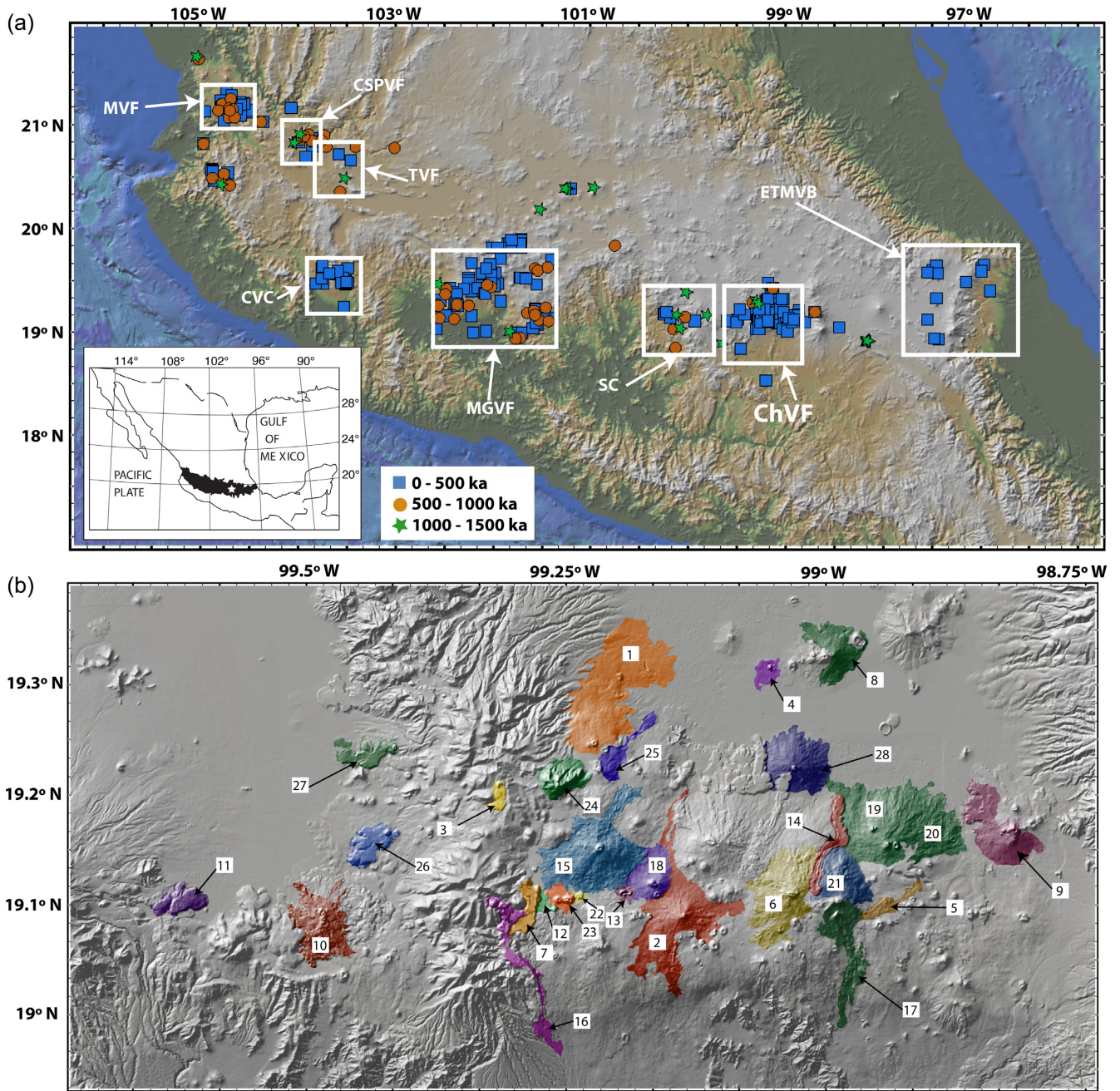


**Figure 1.** (a) TMVB and location of published palaeomagnetic data for the past 1.5 Ma (Satellite image from Google-earth 2018; ChVF: Sierra de Chichinautzin Volcanic Field; CSPVF: Ceboruco-San Pedro Volcanic Field; CVC: Colima Volcanic Complex; ETMVB: Eastern Trans Mexican Volcanic Belt; MGVF: Michoacán-Guanajuato Volcanic Field; MVF: Mascota Volcanic Field; SC: Sierra de las Cruces; TVF: Tequila Volcanic Field). Age references and site locations are available in Table 1S. (b) Coloured areas represent the sampled cooling units in Sierra de Chichinautzin volcanic field and Sierra de Santa Catarina monogenetic volcanic group (numbers refer to the ID of Table 1, location of the sampling sites and age references are available in Table 2; cooling units 4 and 8 belong to the Sierra de Santa Catarina (SSC) volcanic group).

late Pleistocene to Holocene: the Michoacán-Guanajuato Volcanic Field (MGVF, Fig. 1b) in west-central Mexico (e.g. González *et al.* 1997; Michalk *et al.* 2013; Mahgoub *et al.*, 2017, 2019), and the ChVF (Fig. 1b) in central Mexico. There were many palaeomagnetic studies focusing on field directions and intensities, during the last 30 yr (e.g. Herrero-Bervera & Pal 1977; Urrutia-Fucugauchi & Martín Del Pozzo 1993; Böhnell *et al.* 2003; Alva-Valdivia 2005), but new radiocarbon and Argon-Argon ages, obtained in

the past 15 yr (e.g. Siebe *et al.* 2004b, Guilbaud *et al.* 2015; Jaimes-Viera *et al.* 2018) open exciting perspectives for secular variation studies.

In this work, we acquired new palaeomagnetic data from Sierra de Chichinautzin Volcanic Field (ChVF) and Sierra de Santa Catarina (SSC), which were analysed together with previous published data on rocks with well-defined age. Next, a compilation and critical analysis of the available volcanic palaeomagnetic data from

the TMVB improved the understanding of the variation of the geomagnetic field during the late Pleistocene and Holocene in central Mexico.

## 2 GEOLOGY, CHRONOLOGY AND SAMPLING

The TMVB is a volcanic arc, 1000-km-long belt extending from the Pacific Ocean to the Gulf of Mexico, formed by subduction along the Acapulco trench, since middle Miocene (*ca.* 16 Ma) to present day (Ferrari et al., 1994, 1999). The TMVB is roughly a W–E oriented transverse belt, formed by numerous Mexican geological provinces (Ortega-Gutiérrez et al. 1992; Aguirre-Díaz et al. 1998). This geometry exposes a configuration of volcanic vents, which include abundant scoria cones grouped in extensive monogenetic volcanic fields, such as the ChVF (Fig. 1). The variations in the subduction angle of the Cocos plate, chemical assemblages, type of volcanism, change in arc width, and the existence of intraplate subduction-related alkaline volcanism, divide the TMVB into three portions: eastern, central and western (Ferrari et al. 2000; Gómez-Tuena et al. 2007). The scoria cones and related volcanic deposits studied here are part of the central TMVB. During the Pleistocene, more than 8000 volcanic structures, such as stratovolcanoes, scoria and cinder cones, were formed (Demant 1978; Aguirre-Díaz et al. 1998).

The ChVF, a still active hazardous volcanic field, consists of more than 220 monogenetic volcanic structures of wide compositional range. The activity started 1.6 Ma and the last eruption, the Xitle volcano, was dated at 1.6 ka BP (e.g. Martín del Pozzo 1982; Siebe et al. 2004a; Arce et al. 2013). The eruption rate was estimated around  $0.016 \text{ km}^3 \text{ ka}^{-1}$  per  $100 \text{ km}^2$  for the whole volcanic field (Arce et al. 2013) and around  $0.6 \text{ km}^3 \text{ ka}^{-1}$  during the Holocene (Siebe et al. 2005). Close to the ChVF is located the SSC monogenetic volcanic group (units 4 and 8 in Fig. 1b) with seven volcanoes formed by lava flows and pyroclastic deposits, ranging in age from 132 to 2 ka (Jaimes-Viera et al. 2018).

Our palaeomagnetic sampling focused on 21 well-dated volcanic cooling units from the ChVF and SSC (Table 1). A cooling unit is defined here as a volcanic event, during which rocks were emplaced and cooled rapidly, recording almost instantaneously the Earth Magnetic Field. One up to six palaeomagnetic sites have been sampled in a given cooling unit. Ten cooling units were dated using the radiocarbon technique. The uncalibrated ages given in the original papers were carefully analyzed and updated when possible (Table 1). For example, González et al. (1997) reported a  $^{14}\text{C}$  age of  $4070 \pm 150$  uncalibrated BP (Kirianov et al. 1990) for the *El Pelado* volcano but we retained only the three ages,  $9620 \pm 160$ ,  $10\,270 \pm 190$  and  $10\,900 \pm 280$  uncalibrated BP, from Siebe et al. (2004b). All radiocarbon ages were calibrated using the most recent version of the calibration curve Intcal13 (Reimer et al. 2013). The age of seven others cooling units were defined using recent Argon–Argon dates (Arce et al. 2013; Jaimes Viera et al. 2018). Finally, four cooling units could not be dated more precisely than by their stratigraphic constraints with other cooling units.

The sampling was distributed in three groups: (i) the younger group of age ranging from 2 to 40 ka; (ii) the older group of age from 40 ka to 1.2 Ma, sampling volcanic structures and (iii) Sierra de Santa Catarina monogenetic volcanic group. The samples were collected *in situ*, avoiding fractured and displaced blocks. All samples were drilled directly in the field with a portable gasoline powered drill, and oriented with magnetic and sun compasses. A total of

300 cores, one inch in diameter and 6–15 cm long, were collected from 33 individual sites (8–10 cores per site) belonging to 21 cooling units along the ChVF and SSC (Fig. 1b). Cores were cut into 22-mm-long standard specimens.

## 3 METHODOLOGY AND LABORATORY PROCEDURES

Rock magnetic experiments were carried out in the Laboratory of Palaeomagnetism at UNAM, Mexico (except when indicated) to identify the magnetic carriers of magnetization, estimate the thermal stability of the ferromagnetic minerals during the heating processes, and characterize the domain state of the magnetic particles.

One sample per cooling unit was selected to measure the  $k$ – $T$  curves using MFK-FA and MFK2 susceptibility-meters (Agico, Kappabridge) in UNAM and CEREGE laboratories, respectively. Specimens were heated in air from room temperature up to  $620^\circ\text{C}$ .

In order to further investigate the ferromagnetic mineralogy, the hysteresis loops and acquisition of isothermal remanent magnetization (IRM) curves were acquired on small chip rocks from one sample per cooling unit using a Princeton 2900 MicroMag Alternating Gradient Magnetometer, with maximum applied fields up to 1.2 Tesla.

For the determination of the palaeomagnetic directions from the ChVF and SSC, 33 individual sites from 21 different cooling units were studied. Remanent magnetizations were measured using an AGICO JR-6 spinner magnetometer in a magnetically shielded room and analyzed by stepwise alternating field (AF) and/or thermal demagnetization on specimens from all sites. AF demagnetization was carried out on 183 specimens with a Molspin demagnetizer (Molspin Limited, England), using 10 steps up to 100 mT. Thermal demagnetization was performed on 79 specimens in a non-inductive Schönstedt furnace, with 10–12 steps every  $40^\circ\text{C}$  from 100 to  $600^\circ\text{C}$ .

The directions of the Characteristic Remanent Magnetization (ChRM) were estimated by principal component analysis (Kirschvink 1980), with at least five demagnetization steps and a maximum angular deviation (MAD) below  $5^\circ$ . As there are no report of field evidences for local tectonic movements posterior to the lava emplacement, no tectonic correction was applied.

Mean directions and VGPs were calculated at each site with Fisher statistics (Fisher 1953) and summarized in Table 2 with their  $\alpha_{95}$ -confidence circle and Fisher precision parameter ( $k$ ) parameters. A constant VGP latitude of  $45^\circ$  was used as a cutoff to discriminate the transitional values (Tauxe et al. 2003; Johnson et al. 2008; Doubrovine et al. 2019).

## 4 ROCK MAGNETISM

### 4.1 Susceptibility as a function of temperature ( $k$ – $T$ )

After the  $k$ – $T$  experiments, up to 70 per cent of the curves display two magnetic phases during the heating process and high reversibility (Fig. 2a) or a higher susceptibility for the cooling branch.

The Curie temperature range is between  $510$  and  $540^\circ\text{C}$  for the high-temperature phase corresponding to Ti-poor titanomagnetite. The Curie temperature ranging from  $230$  to  $300^\circ\text{C}$ , the low-temperature phase, is likely Ti-rich titanomagnetite. Two samples show highly reversible curves observed with the unique presence of Ti-poor magnetite (Figs 2c and d). The irreversible curve of *El Pelado* (Fig. 2b) might be related to the occurrence of Ti-magnetite

**Table 1.** Summary of the reported ages for ChVF and SSC, including the estimated calibrated age. The radiocarbon ages were calibrated with IntCal13 curve (Reimer *et al.* 2013) using ChronoModel software (Lanos & Philippe 2017). The average age (given in kyr BP) and its error were defined between the older and younger boundaries of the calibrated date interval at 95 per cent of confidence ( $2\sigma$ ).

ID	Cooling unit	Calibrated age (kyrs BP)	Age error (kyrs)	Age method	Uncalibrated $^{14}\text{C}$ (yrs BP)	Reference
1	Xitle	1.61	0.09	$^{14}\text{C}$	1670 $\pm$ 35	Siebe (2000)
2	Chichinautzin	1.75	0.13	$^{14}\text{C}$	1835 $\pm$ 55	Siebe <i>et al.</i> (2004b)
3	Jumento	1.97	0.08	$^{14}\text{C}$	2010 $\pm$ 30	Arce <i>et al.</i> (2015)
4	Guadalupe	2	0.56	Ar-Ar		Jaimes-Viera <i>et al.</i> (2018)
5	Pelagatos	2.6	0.2	$^{14}\text{C}$	2520 $\pm$ 105	Guilbaud <i>et al.</i> (2009)
6	Tlálloc	7.1	0.2	$^{14}\text{C}$	6200 $\pm$ 85	Siebe <i>et al.</i> (2005)
7	Tabaquillo	7	9	Ar-Ar		Jaimes-Viera <i>et al.</i> (2018)
8	Mazatepec	23	4	Ar-Ar		Jaimes-Viera <i>et al.</i> (2018)
9	Chinconquiat	>31		Stratigraphy		
10	Tres Cruces	9.4	0.3	$^{14}\text{C}$	8390 $\pm$ 100 8490 $\pm$ 90	Bloomfield (1975)
11	Tenango Basalt	9.5	1.0	$^{14}\text{C}$	8390 $\pm$ 130 8440 $\pm$ 40 8700 $\pm$ 180	Bloomfield (1974)
12	Los Cardos	<10		Stratigraphy		
13	Cima	10.1	0.6	$^{14}\text{C}$	10 160 $\pm$ 210 10 410 $\pm$ 80	Kirianov <i>et al.</i> (1990)
14	Tlacotenco	6.2–14		Stratigraphy		Siebe <i>et al.</i> (2005)
15	El Pelado	10.8	0.6	$^{14}\text{C}$	9620 $\pm$ 160 10 270 $\pm$ 190 10 900 $\pm$ 280	Siebe <i>et al.</i> (2004b)
16	Huilotte	>10		Stratigraphy		
17	Cerro del Agua	12.6	0.7	$^{14}\text{C}$	10 845 $\pm$ 290	Guilbaud <i>et al.</i> (2015)
18	Acopiexco	>14		Stratigraphy		Lorenzo-Merino (2016)
19	Dos Cerros 1	16.6	0.4	$^{14}\text{C}$	13 695 $\pm$ 110	Guilbaud <i>et al.</i> (2015)
20	Dos Cerros 2	16.6	0.6	$^{14}\text{C}$	13 769 $\pm$ 201	Guilbaud <i>et al.</i> (2015)
21	Cilcuayo	>18.7		Stratigraphy		
22	Raices-Cajete	18.9	0.3	$^{14}\text{C}$		Mahgoub <i>et al.</i> (2019)
23	Tres Cumbres	21.5	1.8	$^{14}\text{C}$	16 700 $\pm$ 150 19 680 $\pm$ 120	Kirianov <i>et al.</i> (1990)
24	Ajusco 1	390	160	K-Ar		Mora-Alvarez <i>et al.</i> (1991)
25	Ajusco 2	22.6	0.3	$^{14}\text{C}$	18 680 $\pm$ 120	Urrutia-Fucugauchi & Martin del Pozzo (1993)
26	Malinale 1	22.8	1.4	$^{14}\text{C}$	18 900 $\pm$ 600	Kirianov <i>et al.</i> (1990)
27	Cuautl	23.5	0.5	$^{14}\text{C}$	19 530 $\pm$ 160	Bloomfield (1975)
28	Tezontle	26.3	0.8	$^{14}\text{C}$	21 860 $\pm$ 540 21 860 $\pm$ 540	Bloomfield (1975)
29	Teuhtli	36	1.8	$^{14}\text{C}$	31 790 $\pm$ 755	Guilbaud <i>et al.</i> (2015)
30	Pueblo Viejo	80	20	Ar-Ar		Arce <i>et al.</i> (2013)
31	Palpan	260	20	Ar-Ar		Arce <i>et al.</i> (2013)
32	Atlacholoaya	1020	160	Ar-Ar		Arce <i>et al.</i> (2013)
33	Villa Guerrero	1200	50	Ar-Ar		Arce <i>et al.</i> (2013)

instead of Ti-magnetite, associated to mineral alteration during the heating-cooling process in the laboratory.

#### 4.2 Hysteresis and IRM curves

The determination of saturation magnetization ( $M_s$ ), saturation remanent magnetization ( $M_{rs}$ ), coercive force ( $H_c$ ) and remanent coercive force ( $H_{cr}$ ) gave information on the domain state of the magnetic grains. With  $M_{rs}/M_s$  ratios between 0.1 and 0.6, and  $H_{cr}/H_c$  between 1.2 and 4.0. 80 per cent of the samples, fit in the pseudo single domain (PSD) field of the Day plot (Day *et al.* 1977), likely indicating a mixture of single domain (SD) and multidomain (MD) grains (Fig. 3b), also evidenced by the wasp-waisted shape of the 09CH007 sample (Fig. 3a). Hysteresis and IRM curves reach saturation above 800 mT, which is consistent with the presence of magnetite with different contents of titanium and the absence of high-coercivity minerals (Fig. 3).

Samples from *El Pelado* and *Chichinautzin* volcano cooling units are close to SD field and those of *Tenango* basalt and *Palpan* cone to MD field.

#### 5 DIRECTIONAL ANALYSIS

We obtained 33 new site directions from ChVF and SSC monogenetic volcanic group: 32 sites are of normal polarity, and one (Villa Guerrero) of reverse polarity (Fig. 5a) with an age at  $1200 \pm 50$  ka (Arce *et al.* 2013), consistent with the Matuyama chron. This is the first reversed polarity reported from the ChVF. After AF and thermal demagnetization, 80 per cent of the samples present a single component of magnetization (Figs 4a and b). The rest of the samples show a secondary component, probably of viscous origin, that could be removed at low field (less than 20 mT; Fig. 4c and d) or low temperature (less than 200 °C; Figs 4e and f). As mentioned before, no structural correction was applied to the samples, as no recent rotation or tectonic displacements were seen in the field or reported in the area in previous published studies (e.g. Herrero-Bervera & Pal 1977; Urrutia-Fucugauchi & Martin del Pozzo 1993).

Values of  $k$  and  $\alpha_{95}$  from all sites range from 68 to 1495 and 2.7° to 8.5°, respectively, underlying the overall high precision and confidence of our mean directions.

**Table 2.** Summary of the directional results, where N is the number of specimens used for the calculation of the mean direction at the site level or the number of sites used for the calculation of the mean direction of the cooling unit, when there is more than six sites in a cooling unit. References: TS, This study (1) Herrero-Bervera & Pal 1977, (2) Urrutia-Fucugauchi & Martin Del Pozzo 1993, (3) González *et al.* 1997, (4) Böhnelt & Molina-Garza 2002, (5) Morales *et al.* 2001, (6) Alva-Valdivia 2005, (7) Vlag *et al.* 2000, (8) Urrutia-Fucugauchi 1996, (9) Böhnelt *et al.* 1997, (10) Mahgoub *et al.* 2019, (11) Mora-Alvarez *et al.* 1991.

ID	Cooling unit	A(ge ka)	Site	Location		N	Dec	Inc	kappa	$\alpha_{95}$	VGP		Ref
				Lat ° N	Long ° W						Plat ° N	Plong ° E	
1	Xitle	1.61 ± 0.09	6	19.300	99.200	17	358	34	301	2.1	88	152	1
			7	19.300	99.200	11	355	34	86	5.0	85	164	1
			11	19.300	99.200	12	16	36	230	2.9	75	346	1
			13	19.300	99.200	8	355	39	114	5.2	85	202	1
			14	19.300	99.200	8	357	52	151	4.5	76	250	1
			15	19.300	99.200	7	356	34	62	7.7	86	162	1
			XT-1	19.180	99.100	6	357	32	276	4.0	87	139	2
			S-9	19.320	99.180	9	350	35	663	2.0	81	172	3
			Xitle	19.190	99.110	15	347	36	521	1.7	78	177	9
			JM	19.320	99.187	13	352	36	269	2.5	82	177	5
			Flow 1	19.315	99.174	9	4	32	87	5.6	86	18	6
			Flow 2	19.315	99.174	8	0	35	351	3.0	90	81	6
			Flow 3	19.315	99.174	10	2	34	131	4.2	88	10	6
			Flow 4	19.315	99.174	10	3	32	156	3.9	87	25	6
			Flow 5	19.315	99.174	8	3	35	72	6.6	87	351	6
			Flow 6	19.315	99.174	9	356	30	309	2.9	85	131	6
			Flow 7	19.315	99.174	9	5	36	280	3.1	85	342	6
			Flow 8*	19.315	99.174	8	359	33	57	7.4	88	117	6
			Xite	19.36	99.17	113	1	34	263	0.8	89	28	4
			Xitle CU-1	19.35	99.13	6	357	34.9	477	3.1	86	17	8
			Xitle CU-2	19.36	99.15	6	353.6	36.2	151	4.5	84	178	8
			Xitle XT-6	19.25	99.26	9	355	37	123	4.7	85	188	8
			Xitle P-8	19.33	99.15	8	356	30	67	6.8	85	131	8
			<b>Average</b>			<b>23</b>	<b>358</b>	<b>35</b>	<b>159</b>	<b>2.4</b>	<b>88</b>	<b>173</b>	
2	Chichinautzin	1.75 ± 0.13	CH-1	19.091	99.080	7	357	30	91	9.7	86	125	TS
			CH-2	19.119	99.126	8	3	30	214	6.3	86	37	TS
			CH-IV	19.105	99.161	8	349	32	181	5.7	79	163	TS
			PL-CH1	19.116	99.147	8	354	34	953	3.0	84	167	TS
			CH-I	19.107	99.156	7	357	40	153	6.2	85	224	TS
			1	19.100	99.100	8	358	27	73	6.5	85	103	1
			GU-PI	19.020	99.140	23	3	34	98	3.1	87	1	10
3	Jumento	1.97 ± 0.08	<b>Average</b>			<b>6</b>	<b>357</b>	<b>32</b>	<b>190</b>	<b>4.4</b>	<b>86</b>	<b>147</b>	
			Jumento	19.206	99.315	16	349	50	233	4.4	75	222	TS
4	Guadalupe	2 ± 0.56	El Jumento—B*	19.187	99.320	25	354	32	52	4.1	84	156	10
			SC1	19.323	99.023	8	9	37	85	6.0	81	341	TS
5	Pelagatos	2.6 ± 0.2	MMA-23-A	19.117	98.910	8	1	27	1459	2.4	85	72	TS
			A2	19.103	98.934	8	3	20	618	3.7	80	61	TS
6	Tlálóc	7.1 ± 0.2	<b>Average</b>			<b>16</b>	<b>2</b>	<b>23</b>	<b>212</b>	<b>3.4</b>	<b>82</b>	<b>66</b>	
			A5	19.140	99.008	7	2	10	180	6.9	76	73	TS
7	Tabaquillo	7 ± 9	Tabaquillo	19.119	99.291	8	360	44	1141	2.7	83	261	TS
8	Mazatepec	23 ± 4	SSC2	19.317	99.036	8	357	34	149	6.3	87	158	TS
9	Chinconquiat	>31	A3	19.207	98.859	8	349	21	209	8.5	77	135	TS
10	Tres Cruces	9.4 ± 0.3	Site 1 + 2	19.103	99.502	16	339	50	196	3.7	68	206	7
			S-6	19.12	99.49	7	337	56	463	3.1	63	216	3
11	Tenango	9.5 ± 1	TEO-Alto	19.110	99.596	8	358	65	163	7.2	62	257	TS
			TEO-Bajo	19.110	99.596	7	3	71	315	5.2	53	263	TS
			<b>Average</b>			<b>15</b>	<b>1</b>	<b>68</b>	<b>137</b>	<b>4.8</b>	<b>58</b>	<b>262</b>	
12	Los Cardos	<10	Tenango1	19.0895	99.6258	10	18	36	99	4.9	73	344	10
			Cardos	19.094	99.260	8	356	39	96	5.6	85	210	TS
13	Cima	10.1 ± 0.6	12*	19.100	99.200	13	6	16	21	9.2	78	52	1
			Cima 2	19.100	99.190	7	17	22	71	7.2	72	14	2
			Cima 3	19.100	99.170	7	355	41	139	5.1	84	215	3
14	Tlacotenco	10.2 ± 3.8	MMA-25-A	19.153	98.983	8	12	12	253	5.8	72	39	TS
			MMA-C	19.161	98.991	7	3	4	238	5.0	73	71	TS
15	El Pelado*	10.8 ± 0.6	<b>Average</b>			<b>15</b>	<b>5</b>	<b>7</b>	<b>143</b>	<b>4.3</b>	<b>73</b>	<b>63</b>	
			SITIO D	19.142	99.169	8	14	22	112	6.4	75	19	TS
			SITIO A	19.116	99.268	6	358	38	79	8.7	87	213	TS
			SITIO B	19.120	99.274	8	347	29	124	6.0	77	156	TS
			SITIO C	19.123	99.277	6	359	38	68	10.5	87	235	TS
			PL-02	19.120	99.260	8	354	34	954	3.0	85	165	TS
			PL-01	19.137	99.255	8	12	22	121	5.4	77	23	TS

Table 2. Continued

ID	Cooling unit	A(ge ka)	Site	Location		VGP							Ref
				Lat ° N	Long ° W	N	Dec	Inc	kappa	$\alpha_{95}$	Plat ° N	Plong ° E	
16	Huiloté	>10	<b>Average</b>			<b>44</b>	<b>0</b>	<b>31</b>	<b>48</b>	<b>6.7</b>	<b>87</b>	<b>81</b>	
			8*	19.200	99.200	9	7	33	51	7.3	83	1	1
			9	19.200	99.200	8	5	27	115	5.2	83	36	1
			10	19.200	99.200	9	6	35	118	4.8	84	349	1
			P-2	19.150	99.210	6	355	15	130	5.9	78	104	2
			S-10	19.140	101.420	7	352	12	60	7.9	75	110	3
			JB	19.186	99.169	8	10	17	198	3.9	76	37	5
			PEL I–II	19.120	99.190	12	18	18	115	4.1	70	18	10
			<b>Average</b>			<b>7</b>	<b>5</b>	<b>23</b>	<b>43</b>	<b>9.3</b>	<b>83</b>	<b>66</b>	
			Huiloté 1	19.034	99.270	8	14	11	353	3.0	71	34	5
			Huiloté 2	19.034	99.304	8	4	23	277	3.3	82	52	5
			A4	19.008	98.985	8	5	17	187	5.6	79	55	TS
			JJ	19.110	99.176	13	353	33	498	1.9	83	162	5
			MMA-46	19.117	98.910	8	2	50	154	6.2	78	270	TS
20	Dos Cerros 2	16.6 ± 0.6	MMA-44	19.156	98.869	8	10	45	174	5.1	78	311	TS
			DCR	19.156	98.868	15	345	48	209	2.7	73	211	10
			MMA-79B	19.139	98.971	8	358	20	223	6.2	81	94	TS
			PI3	19.1058	99.2406	6	359	47	194	4.8	81	255	10
			TC-5	19.100	99.260	6	3	22	317	3.8	82	60	2
			JH	19.19	99.25	8	343	22	371	2.9	72	148	5
			C3-B Ajusco	19.43	99.13	14	0	17	18	9.9	79	81	11
			C3-A Ajusco	19.43	99.13	13	124	0	111	3.8	-32	338	11
			JL	19.22	99.27	10	359	45	131	4.2	83	254	5
			Malinalé 1	19.210	99.210	6	6	33	513	3.0	84	2	2
			S-3	19.220	99.210	5	359	34	175	5.8	89	139	3
			S-7	19.170	99.420	6	343	17	255	4.2	71	141	3
			S-5	19.220	99.470	7	353	64	318	3.4	63	250	3
			A1	19.162	98.991	8	353	31	119	8.5	83	152	TS
28	Teuhtli	36 ± 1.8	5	19.200	99.020	11	345	19	118	4.2	73	140	1
			THT	19.244	99.054	8	355.7	26.5	1066.25	1.7	83.3	120	10
			AT-3	18.527	99.197	8	357	57	636	3.6	71	254	TS
			PA-05	18.843	99.460	8	354	24	387	4.7	82	124	TS
			AT-1	18.689	99.233	8	3	58	227	6.1	70	268	TS
			SH-06	18.894	99.645	7	178	-34	1495	3.2	-88	343	TS
29	Pueblo Viejo	80 ± 20	AT-3	18.527	99.197	8	357	57	636	3.6	71	254	TS
			PA-05	18.843	99.460	8	354	24	387	4.7	82	124	TS
			AT-1	18.689	99.233	8	3	58	227	6.1	70	268	TS
			SH-06	18.894	99.645	7	178	-34	1495	3.2	-88	343	TS

\*Mean direction estimated at site level.

\*Sites that do not fulfill our selection criteria were discarded for the calculation of mean directions.

The cooling units were divided into two groups according to their ages: (i) the younger group of 17 out of the 21 sampled cooling units with ages ranging from 1.7 to 40 ka and (ii) the older group of 4 out of the 21 cooling units with ages ranging from 80 ka to 1.2 Ma. The mean direction associated to the younger group (Dec = 359.7°, Inc = 33.1°, N = 16, k = 22.8,  $\alpha_{95}$  = 7.1°, Plat = 89.6° N, Plong = 205.1° E, K = 37.6,  $A_{95}$  = 6.1), is consistent with the direction of the dipole field (at the average site latitude). The precision interval of K with the 95 per cent confidence (Cox 1969) are ranging from 25 < K < 50. For this estimation, one cooling unit (El Pelado) was discarded for the calculation, because it did not fulfill our selection criteria. The mean direction associated to the older group (Dec = 357.9°, Inc = 49°, N = 4, k = 28.2,  $\alpha_{95}$  = 19.2, Plat = 73.1° N, Plong = 253.8° E, K = 38.8,  $A_{95}$  = 23.8) is pretty similar with a scatter likely related to a larger time interval with only four cooling units available. However, the precision interval of K with the 95 per cent confidence (Cox 1969) is ranging from 6 < K < 39, that is statistically indistinguishable with the younger group. The dispersion of the VGP estimated for this study ( $S_b$  = 13.4) fits with the expected value for the latitude (ca. 20°) according with the Model G (McFadden *et al.* 1991), and with the projections from different data sets at similar latitudes (e.g. Johnson *et al.* 2008; Opdyke *et al.* 2015; Cromwell *et al.* 2018).

## 6 COMPARISON WITH PREVIOUS PUBLISHED DATA FROM ChVF

The ChVF has been previously studied reported by twelve palaeomagnetic studies (Herrero-Bervera & Pal 1977; Mora-Alvarez *et al.* 1991; Urrutia-Fucugauchi & Martin del Pozzo 1993; Mooser *et al.* 1974, 1994; Urrutia-Fucugauchi 1996; Böhnelt *et al.* 1997; Gonzalez *et al.* 1997; Vlag *et al.* 2000; Morales *et al.* 2001; Böhnelt & Molina-Garza 2002; Alva-Valdivia 2005; Maghoub *et al.* 2019) for rocks younger than 40 ka. One of these papers (Mooser *et al.* 1974) was not included in the analysis because important information as the sampling location, age and demagnetization protocols were not given in the publication.

A crucial aspect of such a compilation is the quality of the ages attributed to the different data. When possible, the ages given in the original papers were updated (Table 1). Because it was not possible to attribute them a reliable absolute age, the mean results of *Ajusco* (Morales *et al.* 2001) and the site CH-45 (Urrutia-Fucugauchi & Martin Del Pozzo 1993) had to be discarded. Similar problem occurs with the ages of *Acopiaco* and *Huiloté* from Morales *et al.* (2001), but a relative age could be estimated by stratigraphy according to recent published data, supported by direct observations in the field. Only updated ages by cooling unit are given in Tables 1 and 2.

According to their location and reported age, the previous pub-

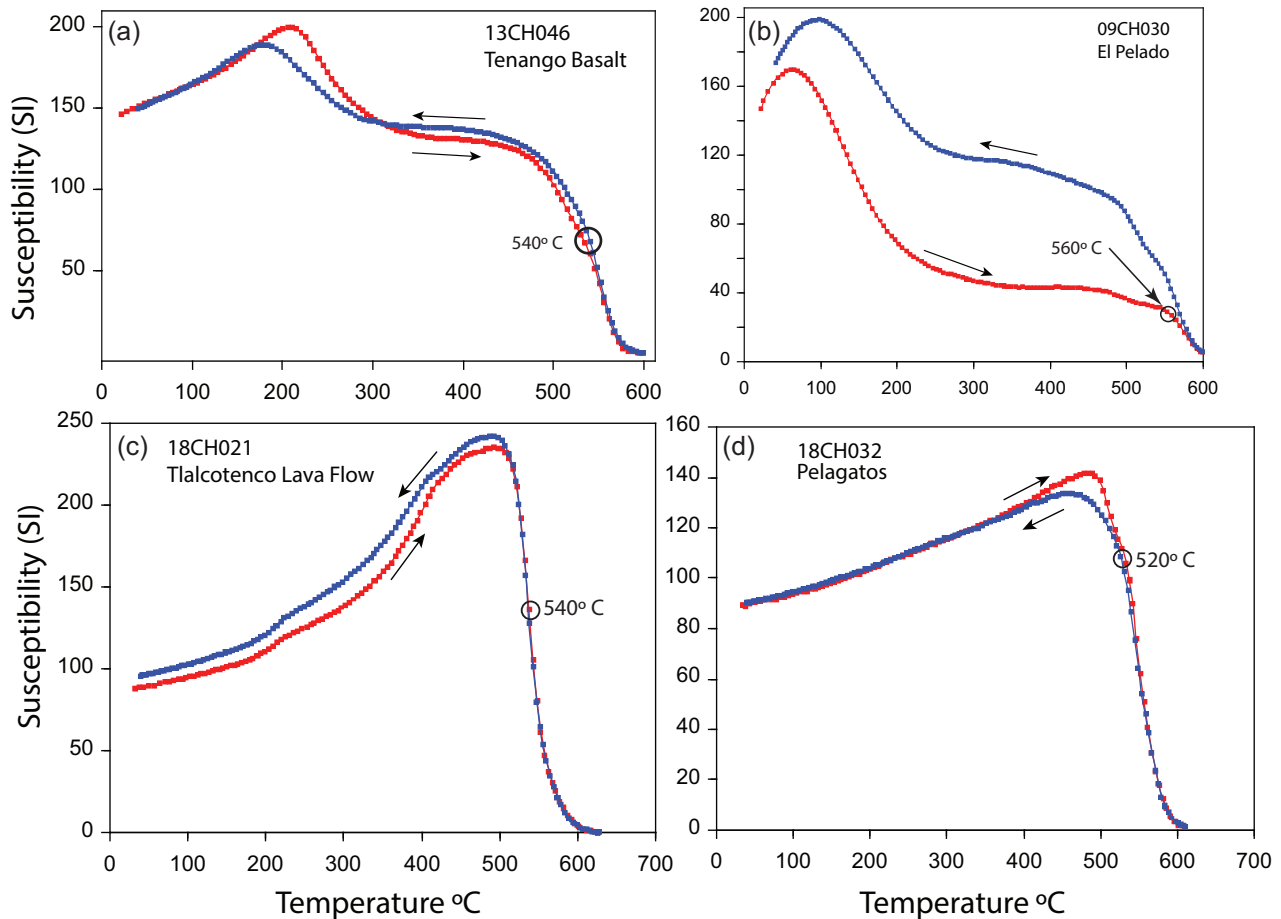


**Figure 2.** Representative heating (red) and cooling (blue) susceptibility vs temperature curves.

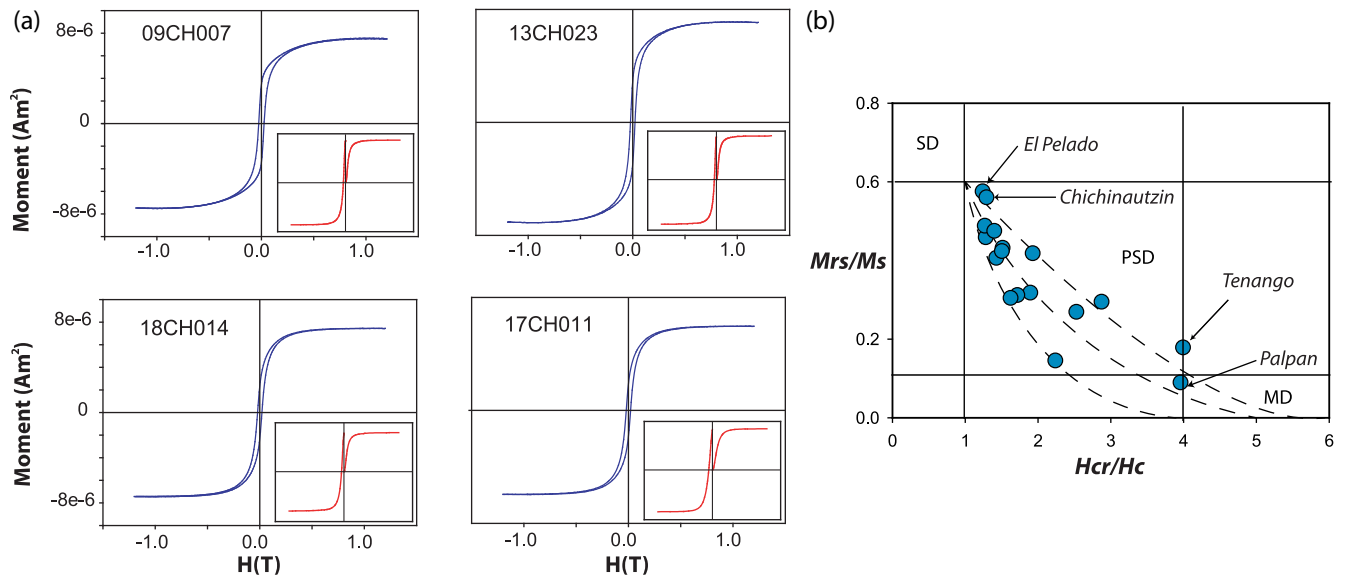


**Figure 3.** (a) Representative hysteresis plots in blue and IRM acquisition and backfield curves in red. Paramagnetic components are removed. (b) Day plot from ChVF and SSC samples with SD-MD mixing curves of Dunlop (2002).

lished mean directions have been allocated to the different ChVF's cooling units (Fig. 1b, Table 2). When different publications report data from the same cooling unit, as for *Xitle* and *El Pelado* volcanoes, we calculate a mean direction at the cooling unit level

(Table 2). For the special case of *El Pelado* volcano, two means are available: a mean estimated at sample level obtained from 44 samples demagnetized in this study obtained for different locations of the volcano; and a mean calculated at site level from 6 sites reported

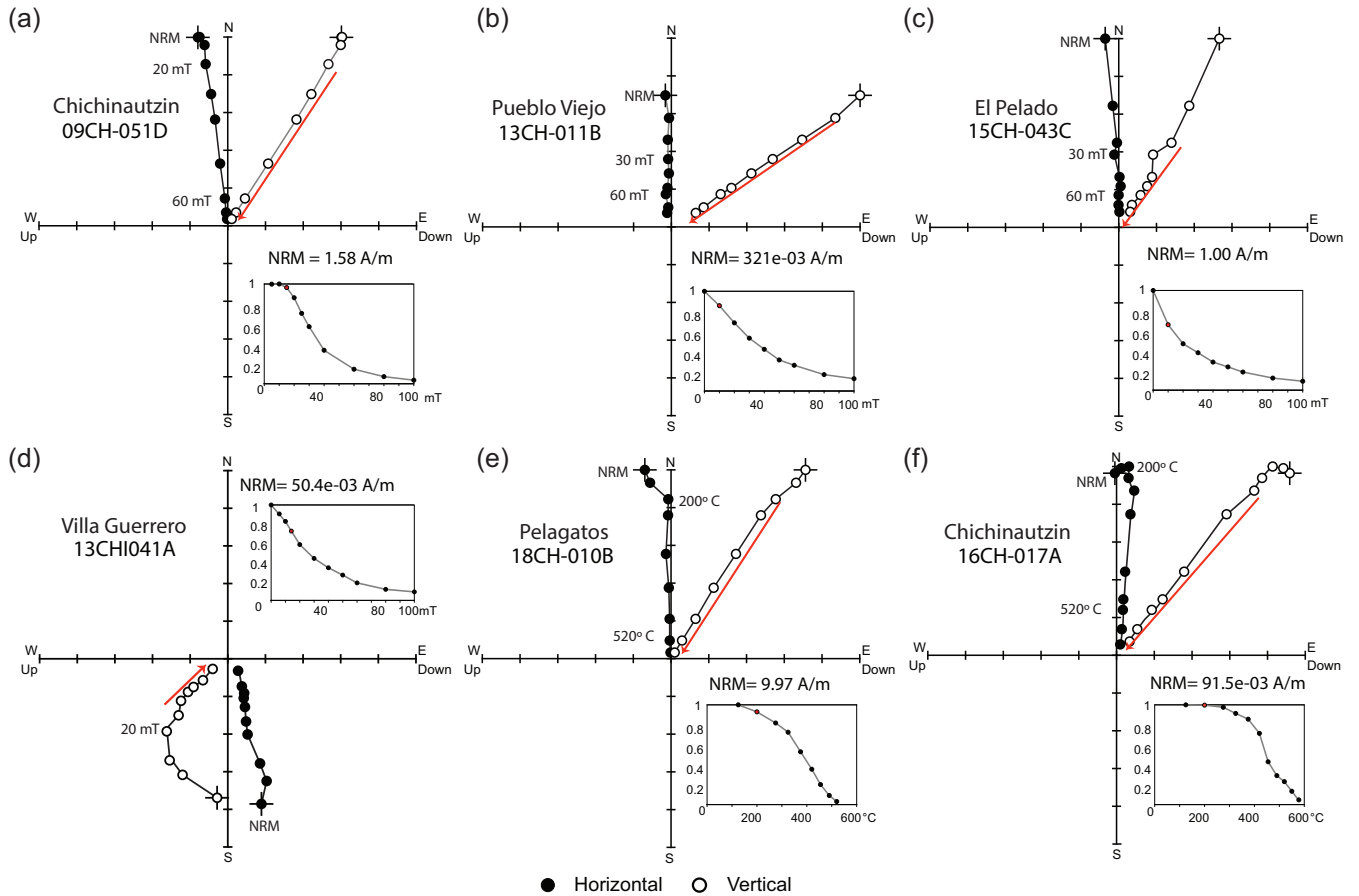


**Figure 4.** Representative orthogonal plots and demagnetization curves of AF (a–d) and thermal (e–f) demagnetization. Solid (open) circles are the projection on the horizontal (vertical) plane. Red line indicates the number of points selected for the ChRM calculation.

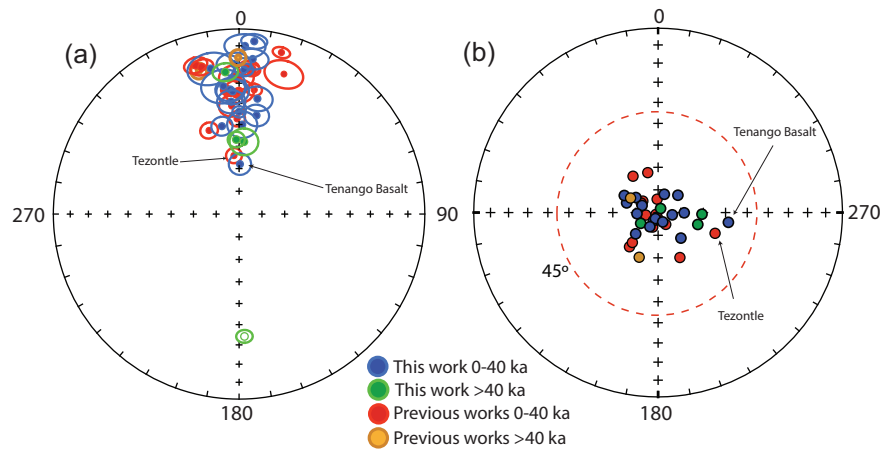


**Figure 5.** Equal area projection of the mean directions (left) and distribution of the VGP's (right) per cooling unit of the ChVF.

from previous works in El Pelado, details available in Table 2. For the previous published data, when more than two sites were available for a given CU, the mean was calculated at site level. When only two sites were available no average was provided, such as Cima volcano, with three sites available, but one of them were discarded. All the mean directions estimated for a given cooling units in this study were calculated at sample level. In order to assure similar quality between our data and the previously published palaeomagnetic data, we defined some minimum quality criteria: at least four

specimens are required to obtain a mean direction for each cooling unit, and cut off value for  $k$  parameter larger than 60 (e.g. Johnson *et al.* 2008; Cromwell *et al.* 2018). This value was determined from the statistical analysis of the directional data compilation from the TMVB on the past 1.5 Ma (Fig. 6) and approaching within 95 per cent confidence of the distribution of the data (ca.  $2\sigma$ ).

A special case is the *Tenango* basalt, located on the western side of the ChVF, of  $8.5 \pm 0.16$  ka (Bloomfield 1974), that presents high value of inclination ( $68.2^\circ$ ), atypical for this period and at

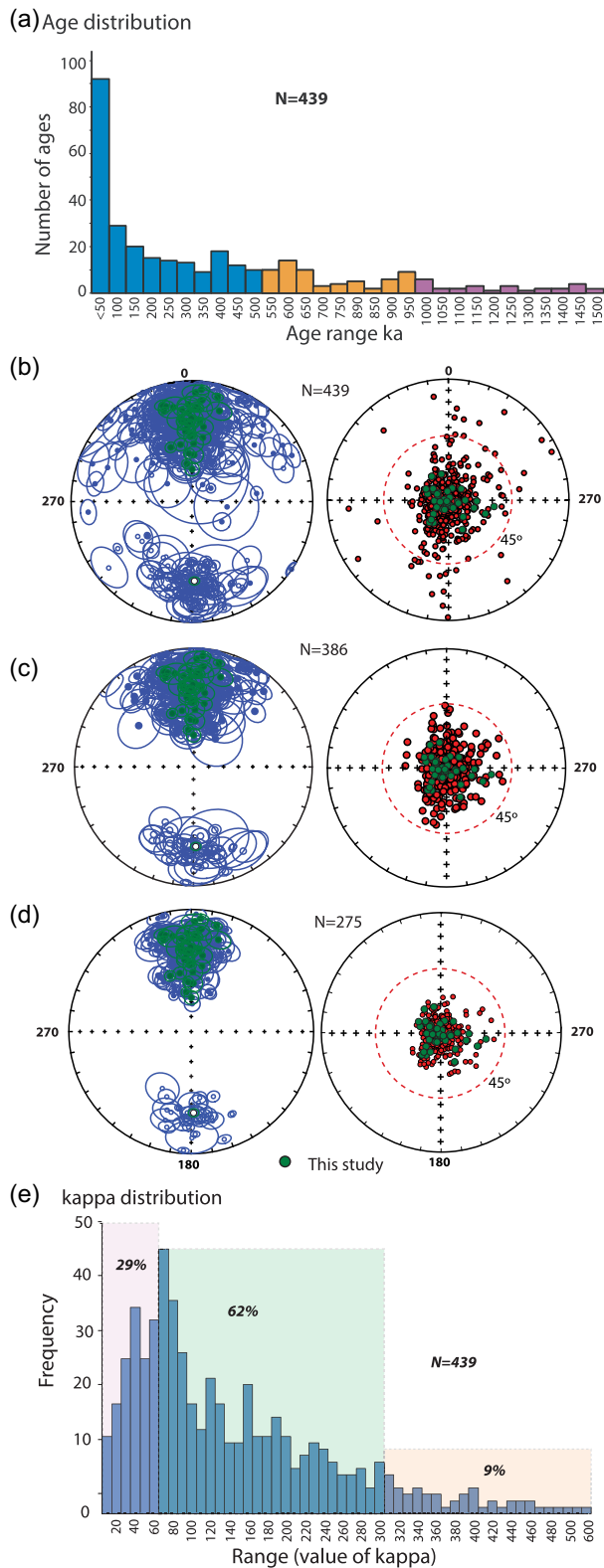


**Figure 6.** Directional relocated data and VGP. (a) Age distribution; (b) all the data in the compilation; (c) after removing data disturbed, transitional or with age problem; (d) after applying quality criteria; (e) distribution of  $k$  for the palaeomagnetic directions of the TMVB for the last 1.5 Ma. Full data set available in Table 1S.

this latitude. Gonzalez *et al.* (1997) report a similar value for the Tezontle volcano ( $21.8 \pm 38$  Ka, Bloomfield 1975), located at the southwestern part of the ChVF. Finally, other two cooling units present similar high inclination values: *Pueblo Viejo* lava flow and *Atlacholaya* scoria cone, both cooling units being located at the southwestern boundary of the volcanic field, but belonging to the older group of the ChVF  $> 40$  ka (Arce *et al.* 2013). On the other side, the cooling unit *Tlálloc*,  $7.1 \pm 0.2$  ka, and the *Tlalcotenco* lava flow, 6.4–14 ka, (Siebe *et al.* 2005) present atypical low inclination value of  $10^\circ$  and  $7^\circ$ , respectively (Table 2). None of these directions can be considered as transitional because they are inside the  $45^\circ$  cut-off (Johnson *et al.* 2008; Cromwell *et al.* 2018) to differentiate transitional polarities (Fig. 5b). According to the statistical quality of the mean directions, there is no objective reason to discard these sites, and they have been included in the mean calculations.

All selected mean directions per cooling unit are presented with their  $\alpha_{95}$  confidence circle in Fig. 5(a), and the associated VGP's in Fig. 5(b). An overall mean was estimated for the last 40 ka (Dec =  $359.1^\circ$ , Inc =  $34.1^\circ$ , N = 30,  $k = 22.2$ ,  $\alpha_{95} = 5.7^\circ$ , Plat =  $88.6^\circ$  N, Plong =  $208.6^\circ$  E, K = 32.4,  $A_{95} = 4.7^\circ$ ). This average is similar to the mean direction that was calculated with our samples, and consistent with the expected value of the actual dipole. The 33 available cooling units for the ChVF and SSC were used to calculate the mean for the last 1.5 Ma (Dec =  $359.1^\circ$ , Inc =  $35.3^\circ$ , N = 33,  $k = 21.6$ ,  $\alpha_{95} = 5.5^\circ$ , Plat =  $87.7^\circ$  N, Plong =  $227.4^\circ$  E, K = 31.8,  $A_{95} = 4.5^\circ$ ) that remains very close to the geographic pole. The overall dispersion of the VGP's estimated ( $S_b = 14.37$ ) of the previous published data combined with the new data set from this study match (Fig. 8) with the predicted value of the Model G (McFadden *et al.* 1991) and with the curves of latitude dependence of VGP scatter published recently (e.g. Johnson *et al.* 2008; Opdyke *et al.* 2015; Cromwell *et al.* 2018), showing an accurately average secular variation recorded from the ChVF lavas.

## 7 THE TMVB PALAEOMAGNETIC DATA SET AND THE TIME AVERAGED DIPOLE FIELD FOR THE LAST 1.5 Ma

The Trans Mexican volcanic belt has been active since the last 12 Ma. However, we restricted our compilation to the last 1.5 Ma, the period for which we have most of the palaeomagnetic studies. 48 publications (Table 1S) were retrieved for this period, most of them are fairly recent (72 per cent of the articles were published in the 2000s), and only a few were published in the 1970s. 30 per cent of the data have an age lower than 50 ka, 20 per cent of the data have ages between 50 and 250 ka, and no trend can be seen between the age distribution and the location (Table 1S).

Around 70 per cent of the previous palaeomagnetic data come from the central part of the TMVB: Michoacán-Guanajuato volcanic field (MGVF); Sierra de la Cruces (SC) and ChVF (Fig. 1b). The latitudes of the data are fairly similar (between  $18.2^\circ$  N and  $21.7^\circ$  N), but the longitudes vary a lot more (from  $96.5^\circ$  W to  $106^\circ$  W) covering about 1000 km from east to west. Therefore, to consider these differences in longitude (up to  $10^\circ$ ), all compiled directions (Table 1S) were relocated to a common geographic place, arbitrarily chosen at Zócalo downtown in Mexico City ( $19.4327^\circ$  N and  $99.1332^\circ$  W).

Altogether 439 individual sites were compiled (Fig. 6b, Table 1S). All data that have been identified by the original authors as remagnetized units, affected by lightning or local tectonics and displaced blocks, or were not considered in the analysis, and are labelled as *disturbed* in Table 1S. Using a  $45^\circ$  cut-off for transitional VGP's,

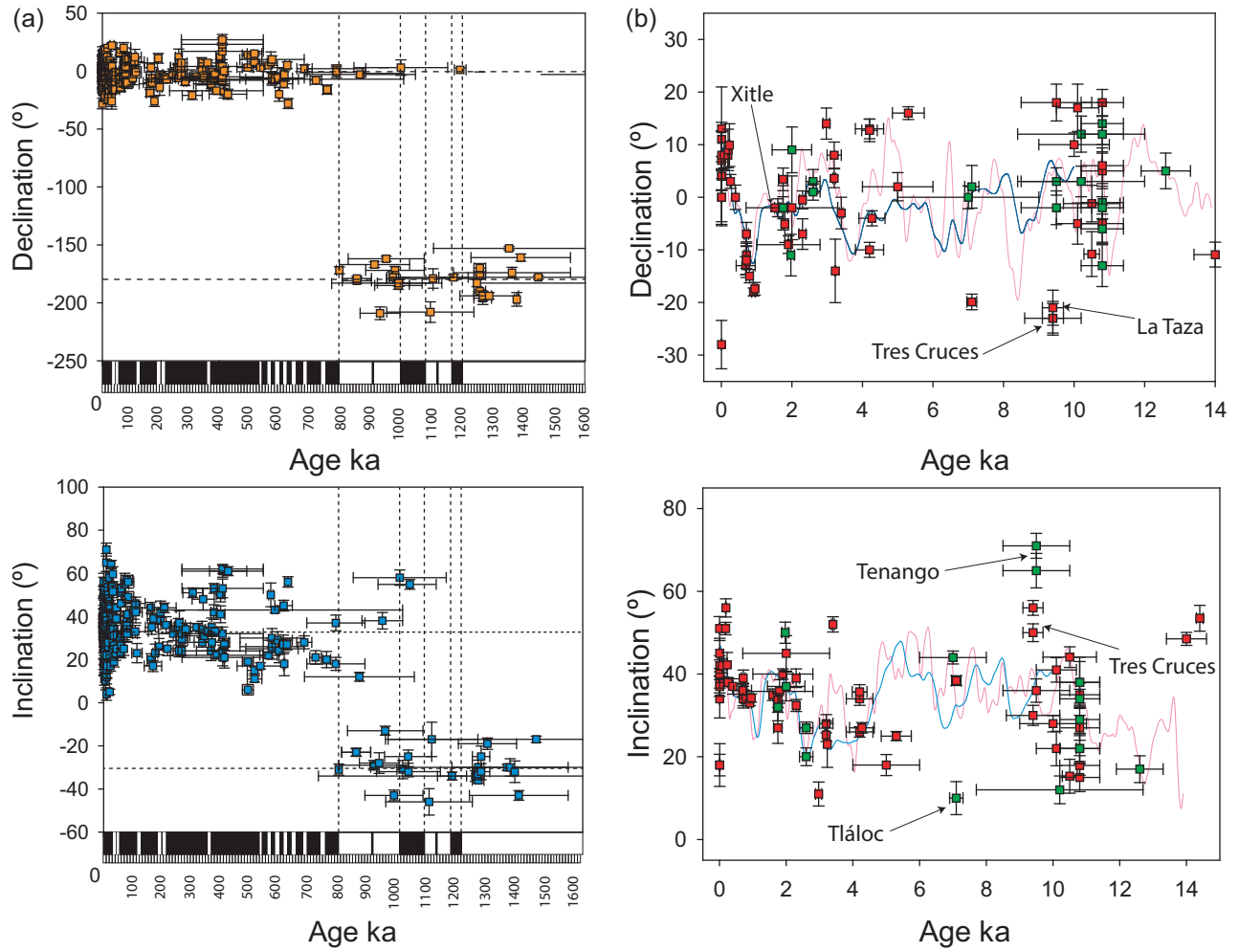


**Figure 7.** a) Distribution of the declination and inclination parameters on the TMVB for the past 1.5 Ma. b) Data from the past 14 ka from ChVF (green squares) and the TMVB (red squares) with the models SHA.DIF.14k (red line) and CALS10k2 (blue line).

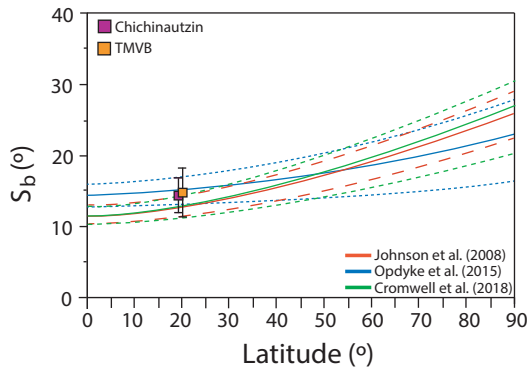


**Figure 8.** Latitude dependence of the VGP's for the last 5 Ma (Johnson *et al.* 2008 and Opdyke *et al.* 2015) and for the last 10 Ma (Cromwell *et al.* 2018). Modified from, Doubrovine *et al.* (2019).

some other data (labelled as *transitional* in Table 1S) were also discarded. The same care was paid to the age of the determination and a certain number of the data were discarded because of imprecision or absence of age (labelled as *age* in Table 1S). After applying these three basic criteria, *ca.* 29 per cent of the data (Fig. 6c) were removed. Finally, the quality criteria used to select the ChVF data ( $N \geq 4$  and  $k > 60$ ) were applied to the TMVB data (Fig. 6d). The

distribution of  $k$  in the published data is summarized in Fig. 6(e), with 29 per cent of the data below the chosen value of 60, 61 per cent of the data having  $k$  ranging from 60 to 300, and 9 per cent of the data with very high-quality value over 300.

An overall mean direction and pole were estimated with the selected palaeomagnetic data set, including the new results from ChVF and SSC. Mean directions were estimated for both normal and reverse polarities, (Dec = 358.4°, Inc = 35°, N = 245,  $k = 31.7$ ,  $\alpha_{95} = 1.5^\circ$ ) and (Dec = 180.6°, Inc = -30.1°, N = 25,  $k = 32.5$ ,  $\alpha_{95} = 5.2^\circ$ ), respectively. The reversal test (McFadden & McElhinny 1990) is positive with a difference of  $\sim 3^\circ$  between the reversal and normal polarities, supporting the reliability of the selected data set. The combined mean direction, calculated for the past 1.5 Ma of the TMVB (Dec = 358.4°, Inc = 35°, N = 275,  $k = 31.7$ ,  $\alpha_{95} = 1.6^\circ$ ) with its corresponding VGP (Plat = 88.3° N, Plong = 188.6° E, K = 40.2,  $A_{95} = 1.4^\circ$ ), is therefore very robust and strongly support the reliability of the Geocentric Axial Dipole hypothesis.

Mexico is indeed characterized by a very active tectonic setting, especially on the west coast with the subduction of the Cocos Plate beneath the North American Plate along the Acapulco trench. The tectonics activity, considered active in the present days make possible local displacements and vertical axis rotations (e.g. Alva-Valdivia *et al.* 2017, 2019), with low influence in the general setting

of all the TMVB. However, if this active tectonic was clearly the trigger of the volcanic activity in central México (Gomez-Tuena *et al.* 2007), no large movement that would have disturbed the TMVB directions could be detected, at least for the last 1.5 Ma. The major tectonic movements along the TMVB were reported for the older activity during the Miocene (Alva-Valdivia *et al.* 2000). It is possible that for the younger activity some areas could be affected by regional tectonic activity, generating tilts and/or vertical axis rotations, the data reported from the authors as tectonically disturbed were not considered for this study. The unrecognized tectonic activity in the area that was not reported by the authors is not possible to observe directly, but the accuracy and precision of the date is supported by the statistical parameters published. The palaeosecular variation (PSV) recorded by the volcanic rocks of the TMVB show that latitude dependence of dispersion of the combined polarities of the VGP's estimated for all the data set in this work ( $S_b = 14.6$ ), show that matches with the different models (e.g. Johnson *et al.* 2008; Opdyke *et al.* 2015; Cromwell *et al.* 2018) at the mean latitude of the TMVB (*ca.* 20°). After discarding the disturbed data from the selection criteria, is possible to determine that the TMVB has a reliable record of the PSV for the last 1.5 Ma. The dispersion of the VGP's show that the local tectonic activity doesn't affect considerably to the mean values estimated in this study (Fig. 8). As reported by Opdyke *et al.* (2015), results from lower latitudes show disturbances on the  $S_b$  due to the intense activity recorded.

Looking at the evolution of relocated declination and inclination through time, we can see that the Brunhes normal chron (0–781 ka) is well recorded in the TMVB data set (Fig. 7a). It is not the same for the Matuyama reverse chron (781–2581 ka), especially during the first reverse subchron (C1r.1r, 781–988 ka) that presents almost as many normal polarity data as reverse polarity data (Fig. 7a). Part of this dispersion is probably due to age uncertainty, but may also be related to undetected remagnetizations in a recent normal field. While the Jaramillo subchron (988–1072 ka) is accurately recorded, the Cobb subchron (1173–1185 ka) is not represented in the TMVB data set.

## 8 SECULAR VARIATION RECORDED IN THE TMVB

Considering the limitations of the available data set, we concentrate on a more recent period, for which we have the larger number of studies, *ca.* 34 per cent of the full data set compiled to study the secular variation: the last 14 millennia (Fig. 7b).

For the last 4 millennia, the TMVB results are consistent with the predictions at Mexico City of two recent global models: CALS10k2 (Constable *et al.* 2016) and SHA.DIF.14k (Pavón-Carrasco *et al.* 2014). This result is not surprising as most data considered in this analysis were included in the calculation of these models. During the last four millennia, declination varied between  $-20^\circ$  and  $20^\circ$  and inclination varied between  $15^\circ$  and  $60^\circ$ .

For earlier periods, the gaps in the database, especially between 5000 and 8000 BP and beyond 11 000 BP, prevent an accurate recovery of the secular variation. The range of directions between 9000 and 11 000 BP suggests a larger and faster secular variation than predicted by the global models. High inclination values up to  $68^\circ$  and low declination values up to  $-30^\circ$  were observed in Tenango, la Taza and Tres Cruces cooling units (Fig. 7b). More data are required to better constrain this large variation and understand its geomagnetic origin.

## 8.1 Dispersion of the VGP's

During the last years, different compilations of directional data from different latitudes around the world, including Mexico were performed (e.g. Johnson *et al.* 2008; Opdyke *et al.* 2015; Cromwell *et al.* 2018; Doubrovine *et al.* 2019). The objective is to assembly the record of the PSV at different intervals of time at different latitudes, showing the dependence of the dispersion of the VGP scatter with the latitude. In this work the dispersion of the VGP was estimated for the ChVF data, and for the data set compiled for the TMVB, to verify the record of the concordance with the Model G (McFadden *et al.* 1991) and with the compilations proposed for the past 0–5 Ma and 0–10 Ma. For Mexico, with a latitude *ca.*  $20^\circ$ , different works estimate the PSV by the VGP scatter for 0–5 Ma. Mejia *et al.* (2005) estimate the VGP scatter ( $S_b = 12.7^\circ$ ) for the TMVB by selecting 187 sites, and found equivalence with the expected value from Model G ( $S_b = 13.5^\circ$ ). Later, Ruiz-Martínez *et al.* (2000) with 77 selected sites, estimated the dispersion of the VGP ( $S_F = 14.8^\circ$ ) and compared the fit with the Model G and the model that use a data set from Mexico ( $S_b = 14.3$ ) proposed by Johnson *et al.* (2008). In this study, we compare the VGP scatter estimated for ChVF ( $S_b = 14.4$ ) and for the entire compilation of TMVB ( $S_b = 14.6$ ), with the results of three global compilations that uses different results from Mexico from 0 to 5 Ma and from 0 to 10 Ma (Cromwell *et al.* 2018). Fig. 8 shows the correspondence of the results from this study with the expected values according with the three models. In the case of Cromwell *et al.* (2018), is possible to observe a slight lower  $S_b$  value, in comparison with the results from the TMVB. This small difference could be associated to a higher average of the model (0–10 Ma). However, in all cases, the results estimated for ChVF and TMVB fit with the expected value of the  $S_b$  according to the latitude. This concurrence, supports the hypothesis that the local tectonic activity in the TMVB does not affect significantly the average estimated for the last 1.5 Ma.

## 9 CONCLUSIONS

The ferromagnetic mineralogy of the ChVF and SSC volcanic groups is dominated by titanomagnetite with different contents in titanium and Curie temperatures ranging from 230 to  $540^\circ\text{C}$ . The magnetic domain state is a mixture of single and multidomain grains.

The directional analysis of the cooling units shows that the mean direction and VGP obtained for the last 40 ka for ChVF are: (Dec =  $359.1^\circ$ , Inc =  $34.1^\circ$ ,  $N = 30$ ,  $k = 22.2$ ,  $\alpha_{95} = 5.7^\circ$ ); and (Plat =  $88.6^\circ$  N, Plong =  $208.6^\circ$  E,  $K = 32.4$ ,  $A_{95} = 4.7^\circ$ ), respectively. These values are close to the present GAD value. The directional results of this study also fit well with the predictions in Mexico City of the global models SHA.DIF.14k and CALS10k2 but only a few data are available from 5 to 9 ka, and study of other structures formed in this time range will be necessary to improve the accuracy of the curves. Similarly, the mean direction and corresponding VGP for the past 1.5 Ma are: (Dec =  $359.1^\circ$ , Inc =  $35.3^\circ$ ,  $N = 33$ ,  $k = 21.6$ ,  $\alpha_{95} = 5.5^\circ$ ); and (Plat =  $87.7^\circ$  N, Plong =  $227.4^\circ$  E,  $K = 31.8$ ,  $A_{95} = 4.5^\circ$ ), respectively, also consistent with the expected GAD value in this period. A reversed polarity dated at  $1020 \pm 160$  (Arce *et al.* 2013) was found, and this is the first geomagnetic reversal recorded by the ChVF.

The mean directions from ChVF and SSC are consistent with the mean directional data recorded in volcanic rocks for all published data from the TMVB (Dec =  $358.4^\circ$ , Inc =  $35^\circ$ ,  $N = 275$ ,  $k = 31.7$ ,  $\alpha_{95} = 1.4^\circ$ ) with its corresponding VGP (Plat =  $88.3^\circ$

N, Plong = 188.6° E, K = 40.2,  $A_{95} = 1.4^\circ$ ). The selection criteria allowed identify the highest quality data to describe the evolution of the time average dipole field, and to constrain the results that will give the most reliable mean directions and VGPs. The directional results and the VGP's scatter (Fig. 8) fit with the expected values according with the latitude of the TMVB, proposed by different global compilations (Johnson *et al.* 2008; Opdyke *et al.* 2015; Cromwell *et al.* 2018). The concordance confirms that the TMVB has not been affected considerably by local tectonics in the past 1.5 Ma. However, large gaps remain in the temporal record of the TMVB that should be filled by further palaeomagnetic studies.

## ACKNOWLEDGEMENTS

We appreciate the financial support to LMAV from PAPIIT-DGAPA-UNAM IN113117 (Mexico), to LMAV and MP from the ANR-CONACyT (France-Mexico) 273564 research projects. GH was supported by Campus France PRESTIGE program (PRESTIGE-2017-1-0002). Thanks to J. A. González Rangel, M. Espinosa, V. Macías and François Demory for their support in the laboratories. The authors would like to thank Dr. A. Biggin (editor), Dr. P. Doubrovine and an anonymous reviewer for their comments.

## REFERENCES

- Aguirre-Díaz, G.J., Ferrari, L., Nelson, S.A., Carrasco-Núñez, G., Lopez-Martínez, M. & Urrutia-Fucugauchi, J., 1998. El cinturón volcánico mexicano: un nuevo proyecto multidisciplinario.
- Alva-Valdivia, L.M., Goguitchaichvili, A., Ferrari, L., Rosas-Elguera, J., Urrutia-Fucugauchi, J. & Zamorano-Orozco, J.J., 2000. Palaeomagnetic data from the Trans-Mexican Volcanic Belt, *Earth, Planets Space*, **52**(7), 467–478.
- Alva-Valdivia, L.M., 2005. Comprehensive paleomagnetic study of a succession of Holocene olivine-basalt flow: Xitle Volcano (Mexico) revisited, *Earth, Planets Space*, **57**(9), 839–853.
- Alva-Valdivia, L.M., Agarwal, A., Caballero-Miranda, C., García-Amador, B.I., Morales-Barrera, W., Rodríguez-Elizarraráz, S. & Rodríguez-Trejo, A., 2017. Paleomagnetic and AMS studies of the El Castillo ignimbrite, central-east Mexico: source and rock magnetic nature, *J. Volc. Geotherm. Res.*, **336**, 140–154.
- Alva-Valdivia, L.M., Agarwal, A., García-Amador, B., Morales-Barrera, W., Agarwal, K.K., Rodríguez, S. & Gonzalez-Rangel, J.A., 2019. Paleomagnetism and tectonics from the late Pliocene to late Pleistocene in the Xalapa monogenetic volcanic field, Veracruz, Mexico, *Bull. geol. Soc. Am.*
- Arce, J.L., Layer, P.W., Lassiter, J.C., Benowitz, J.A., Macías, J.L. & Ramírez-Espinosa, J., 2013. 40 Ar/39 Ar dating, geochemistry, and isotopic analyses of the quaternary Sierra de Chichinautzin volcanic field, south of Mexico City: implications for timing, eruption rate, and distribution of volcanism, *Bull. Volcanol.*, **75**(12), 774.
- Arce, J.L., Muñoz-Salinas, E., Castillo, M. & Salinas, I., 2015. The ~ 2000 yr BP Jumento volcano, one of the youngest edifices of the Sierra de Chichinautzin Volcanic Field, Central Mexico, *J. Volc. Geotherm. Res.*, **308**, 30–38.
- Bloomfield, K., 1975. A late-Quaternary monogenetic volcano field in central Mexico, *Geol. Rundsch.*, **64**(1), 476–497.
- Bloomfield, K., 1974. The age and significance of the Tenango Basalt, central Mexico, *Bull. Volcanol.*, **37**(4), 586–595.
- Böhl, H., Morales, J., Caballero, C., Alva, L., McIntosh, G., Gonzalez, S. & Sherwood, G., 1997. Variation of rock magnetic parameters and paleointensities over a single Holocene lava flow, *J. Geomag. Geoelectr.*, **49**(4), 523–542.
- Böhl, H. & Molina-Garza, R., 2002. Secular variation in Mexico during the last 40,000 years, *Phys. Earth planet. Inter.*, **133**(1–4), 99–109.
- Böhl, H., Biggin, A.J., Walton, D., Shaw, J. & Share, J.A., 2003. Microwave palaeointensities from a recent Mexican lava flow, baked sediments and reheated pottery, *Earth planet. Sci. Lett.*, **214**(1), 221–236.
- Brown, M.C., Donadini, F., Korte, M., Nilsson, A., Korhonen, K., Lodge, A., Lengyel, S.N. & Constable, C.G., 2015. GEOMAGIA50.v3: 1. General structure and modifications to the archeological and volcanic database, *Earth Planets Space*, **67**, 83.
- Constable, C., Korte, M. & Panovska, S., 2016. Persistent high paleosecular variation activity in southern hemisphere for at least 10 000 years, *Earth planet. Sci. Lett.*, **453**, 78–86.
- Cox, A., 1969. Confidence limits for the precision parameter  $\kappa$ , *Geophys. J. Int.*, **17**(5), 545–549.
- Cromwell, G., Johnson, C.L., Tauxe, L., Constable, C.G. & Jarboe, N.A., 2018. PSV10: a global data set for 0–10 Ma time-averaged field and paleosecular variation studies, *Geochem. Geophys. Geosyst.*, **19**(5), 1533–1558.
- Day, R., Fuller, M. & Schmidt, V.A., 1977. Hysteresis properties of titanomagnetites: grain-size and compositional dependence, *Phys. Earth planet. Inter.*, **13**(4), 260–267.
- Del Pozzo, A.M., 1982. Monogenetic vulcanism in sierra Chichinautzin, Mexico, *Bull. Volcanol.*, **45**(1), 9.
- Demant, A., 1978. Características del Eje Neovolcánico Transmexicano y sus problemas de interpretación, *Revista mexicana de ciencias geológicas*, **2**(2), 172–187.
- Doubrovine, P.V., Veikkolainen, T., Pesonen, L.J., Piispa, E., Ots, S., Smirnov, A.V. & Biggin, A.J., 2019. Latitude dependence of geomagnetic paleosecular variation and its relation to the frequency of magnetic reversals: observations from the Cretaceous and Jurassic, *Geochem. Geophys. Geosyst.*, **20**, 1240–1279.
- Dunlop, D.J., 2002. Theory and application of the Day plot (Mrs/Ms versus Hcr/Hc) 2. Application to data for rocks, sediments, and soils, *J. geophys. Res.: Solid Earth*, **107**(B3), EPM 5–1–EPM 5–15.
- Ferrari, L., Garduño, V.H., Pasquare, G. & Tibaldi, A., 1994. Volcanic and tectonic evolution of central Mexico: Oligocene to present, *Geof. Int.*, **33**(1), 91–105.
- Ferrari, L., López-Martínez, M., Aguirre-Díaz, G. & Carrasco-Núñez, G., 1999. Space-time patterns of Cenozoic arc volcanism in central Mexico: From the Sierra Madre Occidental to the Mexican Volcanic Belt, *Geology*, **27**(4), 303–306.
- Ferrari, L., Conticelli, S., Vaggelli, G., Petrone, C.M. & Manetti, P., 2000. Late Miocene volcanism and intra-arc tectonics during the early development of the Trans-Mexican Volcanic Belt, *Tectonophysics*, **318**(1–4), 161–185.
- Fisher, R.A., 1953. Dispersion on a sphere, *Proc. R. Soc. Lond. A*, **217**(1130), 295–305.
- Gómez-Tuena, A., Orozco-Esquivel, M.T. & Ferrari, L., 2007. Igneous petrogenesis of the Trans-Mexican volcanic belt, *Geol. Soc. Am. Spec. Pap.*, **422**, 129–181.
- Gonzalez, S., Sherwood, G., Böhl, H. & Schnepf, E., 1997. Palaeosecular variation in Central Mexico over the last 30000 years: the record from lavas, *Geophys. J. Int.*, **130**(1), 201–219.
- Guilbaud, M.N., Arana-Salinas, L., Siebe, C., Barba-Pingarrón, L.A. & Ortiz, A., 2015. Volcanic stratigraphy of a high-altitude mammothus columbi (Tlacotenco, sierra Chichinautzin), central México, *Bull. Volcanol.*, **77**(3), 17.
- Guilbaud, M.N., Siebe, C. & Agustín-Flores, J., 2009. Eruptive style of the young high-Mg basaltic-andesite Pelagatos scoria cone, southeast of México City, *Bull. Volcanol.*, **71**(8), 859.
- Herrero-Bervera, E. & Pal, S., 1977. Paleomagnetic study of Sierra de Chichinautzin, Mexico, *Geof. Int.*, **17**(2), 167–180.
- Jaimes-Viera, M.C., Martín Del Pozzo, A.L., Layer, P.W., Benowitz, J.A. & Nieto-Torres, A., 2018. Timing the evolution of a monogenetic volcanic field: Sierra Chichinautzin, Central Mexico, *J. Volc. Geotherm. Res.*, **356**, 225–242.
- Johnson, C.L., Constable, C.G., Tauxe, L., Barendregt, R., Brown, L.L., Coe, R.S. & Staudigel, H., 2008. Recent investigations of the 0–5 Ma geomagnetic field recorded by lava flows, *Geochem. Geophys. Geosyst.*, **9**(4).

- Kirianov, V.Y., Koloskov, A.B., De la Cruz, S. & Martin, A.L., 1990. The major stages of manifestation of recent volcanism in the Chichinautzin zone, *USSR Acad. Sci. Geol. Ser.*, **311**, 432–434.
- Kirschvink, J.L., 1980. The least-squares line and plane and the analysis of palaeomagnetic data, *Geophys. J. R. astr. Soc.*, **62**(3), 699–718.
- Lanos, P. & Philippe, A., 2017. Hierarchical Bayesian modelling for combining dates in archaeological context, *J. Soc. Fr. Stat.*, **158**(2), 72–88.
- Lorenzo-Merino, A., 2016. M.s. Thesis. Historia eruptiva del volcán Pelado (Sierra de Chichinautzin, México). Posgrado en Ciencias de la Tierra. Universidad Nacional Autónoma de México, México D.F. México, 89 pp.
- Mahgoub, A.N., Böhnelt, H., Siebe, C. & Chevrel, M.O., 2017. Paleomagnetic study of El Metate shield volcano (Michoacán, Mexico) confirms its monogenetic nature and young age (~ 1250 CE), *J. Volc. Geotherm. Res.*, **336**, 209–218.
- Mahgoub, A.N., Juárez-Arriaga, E., Böhnelt, H., Siebe, C. & Pavón-Carrasco, F.J., 2019. Late-Quaternary secular variation data from Mexican volcanoes, *Earth planet. Sci. Lett.*, **519**, 28–39.
- McFadden, P.L. & McElhinny, M.W., 1990. Classification of the reversal test in palaeomagnetism, *Geophys. J. Int.*, **103**(3), 725–729.
- McFadden, P.L., Merrill, R.T., McElhinny, M.W. & Lee, S., 1991. Reversals of the Earth's magnetic field and temporal variations of the dynamo families, *J. geophys. Res.: Solid Earth*, **96**(B3), 3923–3933.
- Mejia, V., Böhnelt, H., Opdyke, N.D., Ortega-Rivera, M.A., Lee, J.K.W. & Aranda-Gomez, J.J., 2005. Paleosecular variation and time-averaged field recorded in late Pliocene–Holocene lava flows from Mexico, *Geochem. Geophys. Geosyst.*, **6**(7), 2557–2558.
- Michalk, D.M., Böhnelt, H.N., Nowaczyk, N.R., Aguirre-Díaz, G.J., López-Martínez, M., Ownby, S. & Negendank, J.F., 2013. Evidence for geomagnetic excursions recorded in Brunhes and Matuyama Chron lavas from the trans-Mexican volcanic belt, *J. geophys. Res.: Solid Earth*, **118**(6), 2648–2669.
- Mooser, F., Nairn, A.E. & Negendank, J.F., 1974. Palaeomagnetic investigations of the tertiary and quaternary igneous rocks: VIII a palaeomagnetic and petrologic study of volcanics of the valley of Mexico, *Geol. Rundsch.*, **63**(2), 451–483.
- Mora Álvarez, G., Caballero Miranda, C., Urrutia Fucugauchi, J. & Uchiumi, S., 1991. Southward migration of volcanic activity in the Sierra de Las Cruces, basin of Mexico—a preliminary K–Ar dating and palaeomagnetic study, *Geof. Int.*, **30**(2), 61–70.
- Morales, J., Goguitchaichvili, A. & Urrutia-Fucugauchi, J., 2001. A rock-magnetic and paleointensity study of some Mexican volcanic lava flows during the Latest Pleistocene to the Holocene, *Earth, Planets Space*, **53**(9), 893–902.
- Opdyke, N.D., Kent, D.V., Foster, D.A. & Huang, K., 2015. Paleomagnetism of Miocene volcanics on Sao Tome: Paleosecular variation at the Equator and a comparison to its latitudinal dependence over the last 5 Myr, *Geochem. Geophys. Geosyst.*, **16**(11), 3870–3882.
- Ortega-Gutiérrez, F., Mitre-Salazar, L.M. & Roldan-Quintana, J., 1992. Carta geológica de la República Mexicana. Consejo de Recursos Minerales y en el Instituto de Geología de la UNAM.
- Panovska, S., Constable, C.G. & Brown, M.C., 2018. Global and regional assessments of paleosecular variation activity over the past 100 ka, *Geochem. Geophys. Geosyst.*, **19**, 1559–1580.
- Pavón-Carrasco, F.J., Osete, M.L., Torta, J.M. & De Santis, A., 2014. A geomagnetic field model for the Holocene based on archaeomagnetic and lava flow data, *Earth planet. Sci. Lett.*, **388**, 98–109.
- Reimer, P.J. et al., 2013. IntCal13 and Marine13 Radiocarbon Age Calibration Curves 0–50,000 Years cal BP, *Radiocarbon*, **55**(4), 1869–1887.
- Ruiz-Martínez, V.C., Osete, M.L., Vegas, R., Nunez-Aguilar, J.I., Urrutia-Fucugauchi, J. & Tarling, D.H., 2000. Palaeomagnetism of Late Miocene to Quaternary volcanics from the eastern segment of the Trans-Mexican Volcanic Belt, *Tectonophysics*, **318**(1–4), 217–233.
- Siebe, C., 2000. Age and archaeological implications of Xitle volcano, southwestern Basin of Mexico-City, *J. Volc. Geotherm. Res.*, **104**(1–4), 45–64.
- Siebe, C., Rodríguez-Lara, V., Schaaf, P. & Abrams, M., 2004a. Radiocarbon ages of Holocene Pelado, Guespalapa, and Chichinautzin scoria cones, south of Mexico City: implications for archaeology and future hazards, *Bull. Volcanol.*, **66**(3), 203–225.
- Siebe, C., Rodri', V., Schaaf, P. & Abrams, M., 2004b. Geochemistry, Sr–Nd isotope composition, and tectonic setting of Holocene Pelado, Guespalapa and Chichinautzin scoria cones, south of Mexico City, *J. Volc. Geotherm. Res.*, **130**(3), 197–226.
- Siebe, C., Arana-Salinas, L. & Abrams, M., 2005. Geology and radiocarbon ages of Tlálloc, Tlacotenco, Cuauhtzin, Hijo del Cuauhtzin, Teuhtli, and Ocusacayo monogenetic volcanoes in the central part of the Sierra Chichinautzin, México, *J. Volc. Geotherm. Res.*, **141**(3–4), 225–243.
- Tauxe, L., Constable, C., Johnson, C.L., Koppers, A.A., Miller, W.R. & Staudigel, H., 2003. Paleomagnetism of the southwestern USA recorded by 0–5 Ma igneous rocks, *Geochem. Geophys. Geosyst.*, **4**(4).
- Urrutia-Fucugauchi, J., 1996. Palaeomagnetic study of the Xitle-Pedregal de San Angel lava flow, southern Basin of Mexico, *Phys. Earth planet. Inter.*, **97**(1–4), 177–196.
- Urrutia-Fucugauchi, J. & Martín del Pozzo, A.L., 1993. Implicaciones de los datos paleomagnéticos sobre la edad de la Sierra de Chichinautzin, cuenca de México, *Geof. Int.*, **32**(3), 523–533.
- Vlag, P., Alva-Valdivia, L., De Boer, C.B., Gonzalez, S. & Urrutia-Fucugauchi, J., 2000. A rock-and paleomagnetic study of a Holocene lava flow in Central Mexico, *Phys. Earth planet. Inter.*, **118**(3), 259–272.

## SUPPORTING INFORMATION

Supplementary data are available at [GJI](#) online.

Table 1S: Compilation of volcanic data from the TransMexican Volcanic Belt over the last 1.5 Myr

Please note: Oxford University Press is not responsible for the content or functionality of any supporting materials supplied by the authors. Any queries (other than missing material) should be directed to the corresponding author for the paper.